

Proton total reaction cross section measurements for $^{40,44,48}\text{Ca}$ at 700 MeV

B. D. Anderson

Case Western Reserve University, Cleveland, Ohio 44106
and Kent State University, Kent, Ohio 44242

P. R. Bevington, F. H. Cverna,* M. W. McNaughton, and H. B. Willard

Case Western Reserve University, Cleveland, Ohio 44106

R. J. Barrett and N. S. P. King

Los Alamos Scientific Laboratory, Los Alamos, New Mexico 87545

D. J. Ernst

Texas A.&M. University, College Station, Texas 77843

(Received 1 August 1978)

Proton total reaction cross sections for 700 MeV protons on $^{40,44,48}\text{Ca}$ have been measured by detecting inelastically scattered particles at angles greater than 10° (lab). The measurements were performed with overall uncertainties of $\pm 6.2\%$ and relative uncertainties of $\pm 2.5\%$. These measurements yield the values of $\sigma_R(^{40}\text{Ca}) = 614$ mb, $\sigma_R(^{44}\text{Ca}) = 643$ mb, and $\sigma_R(^{48}\text{Ca}) = 736$ mb. Matter radii differences $\Delta(44-40) = (0.05 \pm 0.09)\text{fm}$ and $\Delta(48-40) = (0.36 \pm 0.09)\text{fm}$ were extracted based on a theoretical calculation which takes advantage of the geometrical nature of the cross section. The results are compared to other available measurements of total reaction cross sections on medium-weight nuclei at medium energies and to other determinations of the matter radii differences for the calcium isotopes.

[NUCLEAR STRUCTURE $^{40,44,48}\text{Ca}$; measured proton total reaction cross sections, $E=700$ MeV. Deduced matter radii differences.]

I. INTRODUCTION

We report here measurements of the total reaction cross sections for 700 MeV protons incident upon ^{40}Ca , ^{44}Ca , and ^{48}Ca nuclei. Besides providing further tests of the various nucleon-nucleus reaction models, new measurements of total reaction cross sections may also serve to determine the change in nuclear-matter radii of different isotopes of an element. Medium- and heavy-weight nuclei are known to be strongly absorbing for medium-energy projectiles,¹ and earlier experiments have demonstrated convincingly that a description of nucleon-nucleus scattering in terms of an "opaque disk" model is amazingly accurate, especially for describing the total reaction cross section.^{2,3} Because nuclei are so strongly absorbing and because the de Broglie wavelength of a medium-energy nucleon projectile is small compared to the average internucleon spacing in a nucleus, the total reaction cross section of different isotopes of the same element will vary to a first approximation as the square of the radius of nuclear matter, R_m . This simple R_m^2 dependence has been observed as a general trend over the entire range of the periodic table in earlier experimental results.^{4,5}

The relation of the total reaction cross section

to nuclear size in Refs. 2-5 was derived using optical arguments. Such a relationship is more general, however, and arises also from the approach of Glauber¹ or from the use of an optical potential together with an eikonal approximation for the propagator.⁶ These latter approaches, which allow one to make corrections to the results of Refs. 2-5 for the finite size of the nucleon-nucleon interaction and recent advances in systematically estimating corrections to eikonal approximations,⁷ allow one to relate the total reaction cross section to the rms matter radius of the target nucleus in a quantitative way. Even though this relation may be somewhat model dependent, one feels particularly confident in using such measurements to look for *changes* in nuclear sizes. To this end, we have performed measurements of the total reaction cross sections for three isotopes of calcium. Although measurements of total reaction cross sections for medium-energy protons on various nuclei have been reported earlier,^{4,5} they have been performed only with natural targets or only for one isotope of an element. We believe this experiment represents the first measurements of the total reaction cross section on more than one isotope of an element for medium-energy protons.

II. EXPERIMENTAL PROCEDURE

A floor plan of the experimental arrangement is shown in Fig. 1. The external proton beam (EPB) from the Los Alamos Meson Physics Facility (LAMPF) with an energy of 800 MeV (± 8 MeV) was focused on a 2-cm-long liquid hydrogen target to a spot size approximately 3 mm in diameter and with an emittance less than 1 mr cm. After passing through the target, the beam proceeded some 20 m downstream to a Faraday cup/beam stop. An ion chamber or secondary emission monitor could be introduced to intercept the beam about 8 m downstream from the target. The liquid hydrogen target cell was made of 0.051 mm Kapton and was enclosed in a scattering chamber with 0.051 mm Mylar windows.

Protons elastically scattered by hydrogen nuclei in the target to an angle of 17.5° with an energy of 700 MeV (± 7 MeV) were collimated by a $5\text{ cm} \times 5\text{ cm}$ aperture in 40 cm of lead and allowed to strike a calcium target 4.1 m from the center of the liquid hydrogen target. The elastically scattered protons were detected by a pair of multiwire proportional chambers $16 \times 16\text{ cm}^2$ immediately in front of the calcium target in coincidence with the conjugate protons scattered at an angle of 65.5° detected by another pair of multiwire chambers $16 \times 16\text{ cm}^2$ at a distance of 2.6 m from the center of the liquid hydrogen target. Both pairs of multiwire chambers had anode wire spacings of 2.5 mm and provided identification of the elastically scattered protons to better than 0.2° in both opening angle (θ) and for coplanarity (ϕ). The method used here to identify elastically scattered protons was used earlier to measure the absolute differential cross sections for proton-proton scattering at 647 and 800 MeV,⁸ where the experimental apparatus and techniques are described in more detail.

The number of 700 MeV protons incident on a calcium target was just the sum of events inside the θ - ϕ windows set around the elastically scat-

tered peak. Thus, the incident protons were counted individually. The calcium targets were 3.18 cm in diam. and about 0.9 cm thick. About 1% of the incident protons interacted inelastically and scattered in the calcium target. Any charged particles produced in such an interaction were then detected by a third pair of multiwire chambers $32 \times 32\text{ cm}^2$ located about 12 cm behind the target. The experimental measurements were of angular distributions of all emitted charged particles within the solid angle ($\leq 60^\circ$) subtended by the multiwire chambers behind the target. Because the time resolution of the multiwire chambers was only about 30–40 ns, multiple charged-particles from one incident proton could not be resolved. Such multiple events were tagged electronically by the data-acquisition system, before the event was stored on magnetic tape. Proton interactions in the calcium target which produced only a neutral particle could not be counted with this apparatus. The single reaction channel which produces only a neutral particle in the final state is the (p, n) reaction and has been estimated by Bertini *et al.*⁹ to be about 2% of the total reaction cross section for 660 MeV protons on medium-weight nuclei. Thus, the inability to detect this one channel will introduce a small error in the absolute values for the total reaction cross sections, but will not significantly affect the comparisons between the different isotopes.

A. Scaling incident protons

Since the number of incident protons is actually determined by events seen with the multiwire chambers in front of the calcium target in coincidence with the conjugate particle chamber pair, any inefficiencies in these chambers, or dead time of the system to events closely spaced in time, serves only to reduce the number of accepted incident protons. Scattered particles produced in the calcium target by incident protons not counted for these reasons, will not be analyzed since the system is gated on only when a valid incident proton is accepted.

B. Data acquisition

The design and operating characteristics of the multiwire proportional chambers have been described elsewhere.¹⁰ A digital readout system for the multiwire chambers which had originally been developed for measurements of proton-proton scattering was extended for these measurements.¹¹ Events with multiple wires firing in a chamber could be located and read out or just tagged. Only events with single hits in the two pairs of multi-

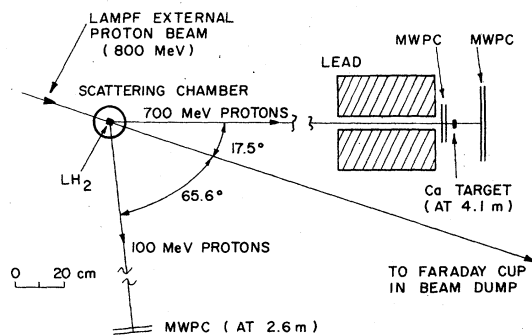


FIG. 1. Floor plan of the experimental arrangement.

wire chambers used to identify elastically scattered protons from the liquid hydrogen target were considered. This eliminated any uncertainty about the position of a proton incident upon the calcium target (to within the wire spacing of the chambers) and only slightly reduced the incident proton rate. Compound events in the larger chamber pair behind the calcium target were tagged and sorted out later as described below.

In order for an event to be valid, it had to be detected in the larger pair of multiwire chambers behind the target as well as be inside the θ - ϕ windows determined by the other two pairs of chambers. This requirement was valid both for events which produced a scattered charged particle in the calcium target and for unscattered protons. Since the efficiency of the large pair of chambers was slightly less than unity, this requirement again slightly reduced the valid count rate, but had the strong advantage of eliminating the uncertainty in knowing the exact efficiency for the large chambers. This requirement also allowed for a tighter coincidence time between all three pairs of chambers to minimize the accidental coincidence rate. Finally, requiring that an event be detected in all three pairs of chambers in order to be valid also eliminated any correction for dead time. Incident protons were completely ignored if the entire system was not ready to detect particles.

Events which satisfied the coincidence requirements had their addresses encoded and stored in input register CAMAC modules. Data in the input registers were transferred to a buffer in the CAMAC microprogrammed branch driver (MBD) and then through priority interrupt to the PDP-11/45 computer for storage on magnetic tape. Between events the computer accumulated and displayed histograms of chamber counts, distributions in the opening angle θ and coplanarity ϕ , and the angle of scatter in the calcium target. The chamber histograms allowed each chamber to be continuously monitored for bad wires, noisy spots, and relative efficiencies. The scattering angle histograms provided a simple on-line analysis to monitor the quality of the data.

C. Data taking

The total number of incident protons varied from 1.5 to 1.7×10^6 for each of the three isotopes of calcium studied. Total target-in run times of about 12 hours were required for each target. Target-out runs were performed for each target for about one-half the number of incident protons as for target-in runs. The data for each isotope were accumulated in six or seven separate ex-

perimental runs each, with target-out runs performed between the target-in runs.

III. DATA REDUCTION

The total reaction cross section for each isotope was determined in these experiments by integrating over angle the measured angular distribution of inelastically produced charged-particles. Since elastic-scattering dominates at small angles, the measurements of inelastic particles could only be performed reliably from about 10° (lab) outward and the integration of the reaction cross section had to be extrapolated to 0° . This extrapolation and its uncertainty are discussed more fully below. The number of particles $N_S(\theta)$ scattered at angle θ into an interval of solid angle $\Delta\Omega$, by a target of n_i nuclei per cm^2 , is related to the total number of incident protons N_i by the differential cross section $\sigma(\theta)$ in the usual way:

$$N_S(\theta) = N_i n_i \overline{\sigma(\theta) \Delta\Omega},$$

where the cross section average is taken over the finite solid angle interval set by the experimental conditions. The measurements of all parameters required to calculate the differential cross sections together with the integration and extrapolation to obtain the total reaction cross sections are discussed in the following subsections.

A. Incident number of protons N_i

The dominant uncertainty in the number of incident protons N_i is due to the contamination of the valid events accepted as incident protons by other particles or protons of other energies. The high spatial resolution of the multiwire chambers combined with the small spot size of the 800 MeV proton beam on the liquid hydrogen target, provides a very sharp peak with very little background in the spectrum of opening angle θ versus coplanarity ϕ for the forward and conjugate scattered protons. Essentially all background events that were not just proton-proton scattering were eliminated by narrow windows on the θ - ϕ peak. The majority of the background in the acceptance region is protons from quasifree scattering of the proton beam with nucleons inside heavier nuclei of the liquid-hydrogen target walls, which should have very close to the same energy (700 MeV) under the θ - ϕ peak as free proton-proton scattering. Since the background under the elastic-scattered peak was observed to be about 1% of the peak area, we estimate the contamination to be less than $\pm 0.5\%$ and take this to be the uncertainty in the number of incident protons.

B. Target thickness n_t

Each calcium target was 3.18 cm in diameter by about 0.9 cm thick, covered with a $397 \mu\text{g}/\text{cm}^2$ layer of aluminum to prevent oxidation. The areal density of each target was determined from measurements of their dimensions and by weighing to an accuracy of $\pm 0.5\%$. The enrichments of the three targets were: ^{40}Ca —99.96%, ^{44}Ca —98.44%, and ^{48}Ca —94.47% with isotopic purities accurate to $\pm 0.05\%$. Essentially all of the impurity in the ^{44}Ca and ^{48}Ca targets was ^{40}Ca . The isotopic and spectrographic analyses were provided by the Isotope Sales Division of the Oak Ridge National Laboratory and the measurements of sizes and weights were performed at the Los Alamos Scientific Laboratory.

C. Solid angle $\Delta\Omega$

The solid angle interval $\Delta\Omega$ within which the reaction products from proton interactions in the calcium targets were counted was determined by setting windows on the radius of scatter observed in the large pair of multiwire chambers located behind the target. The alignment of the pair of chambers behind the target to the pair of chambers immediately in front of the target was performed empirically to better than one-half of a wire spacing (i.e., to better than 1.2 mm) by noting the correspondence of proton events in the two chamber pairs with no calcium target in the holder. The difference in X and Y coordinates (ΔX , ΔY) between the chamber pair in front of the target and the large chamber pair 12 cm behind the target were determined for each event and the radius of scatter calculated. The data were binned for analysis by this radius of scatter parameter, IRAD. If a proton was unscattered by the calcium sample, the radius of scatter was zero and IRAD = 1. The largest scattering angle which could be detected (62°) was to a corner of the large multiwire chamber pair and had a radius of scatter of 22.6 cm or IRAD = 45. The angular resolution varied from about 1.2° at a scattering angle near 0° to about 0.6° at a scattering angle near 60° .

The uncertainty in the solid angles subtended arises from the uncertainties in the distance from the point of interaction in the calcium target to the anode wire locations in the large multiwire chamber pair behind the target and from the variation in wire spacings across the chambers. Since a large number of wire spacings are included for the calculation of $\Delta\Omega$ for each value of IRAD, and since the incident protons will interact uniformly across the thickness of the calcium target, both of these uncertainties average out. The appropriate distances were measured to an accuracy of

± 0.05 cm and the resultant uncertainty in the solid angles is about 0.4%.

D. Number of scattered particles $N_s(\theta)$

The number of scattered particles $N_s(\theta)$ is the total number of events recorded in each bin of IRAD, the radius of scattering parameter. The value of IRAD was determined for each event from its ΔX and ΔY coordinate values. Inspection of the ΔX - ΔY plane for scattered events, even after target-out run subtractions, revealed certain difficulties.

First, if two or more charged particles were produced by one incident proton in a calcium target, two or more X and Y wires would be triggered in the large multiwire chamber pair behind the target. Since the chambers were always read out in the same direction, the lowest number wires in the X and Y planes were always read out first and taken to be the coordinates of scatter. The first quadrant of the ΔX - ΔY plane was overpopulated from events which produced two or more charged particles and the read-out system provided a biased resolution of the ambiguity regarding which ΔX - ΔY set of coordinates to assign to such multiple events. The important criterion, however, for the integrated total reaction cross section is just that the event be counted *somewhere* (and only once).

The ΔX - ΔY spectra also revealed "roots" along the axes corresponding to $\Delta X = 0$ or $\Delta Y = 0$ for one of the scattering-coordinate values. These events were tagged as multiple-hit events and represent events where one of the two particles detected corresponds to an unscattered event. Inspection of the various combinations of ΔX - ΔY coordinates for these events show that many of these events had a combination which corresponded to an unscattered event. That some of the remaining events in these roots did not have a combination which corresponded to an unscattered event was apparently due to the fact that many particles traversing a chamber will do so somewhat obliquely and will fire two or more adjacent wires. Unfortunately, our system tagged such events as multiple-hit events and would read out only those first two adjacent wire locations for that chamber. If the event was also a true multiple event, the correct wire address for the second event was not recorded (since only two addresses from each chamber were recorded). The events remaining in the "roots" of the ΔX - ΔY spectra were determined to be unscattered protons plus δ rays (scattered electrons) from the calcium target. Those events in the roots with no coordinate combination corresponding to an unscattered pro-

ton were δ rays which fired two (or more) adjacent wires in one of the two planes of the large multi-wire chamber pair. These δ -ray events were rejected in the data analysis by eliminating the root regions in the ΔX - ΔY plane before forming the angular distributions. This was performed for several different sized root regions in order to verify that the final determination of the total reaction cross section remained constant once the roots were made large enough.

There remained one more difficulty in the determination of $N_s(\theta)$ from the ΔX - ΔY spectra due to the presence of δ rays. Part of the overpopulation in the first quadrant could also be just δ rays and not necessarily a true multiple event. The first quadrant could not simply be eliminated from the analysis since that would result in the loss of many true multiple events. The differences in the total reaction cross sections determined with and without including the first quadrant of the ΔX - ΔY plane were typically 20%. By studying the relative populations of the four different quadrants and the root regions, we estimate that about one-half of the increase is due to true multiple events from proton interactions in the calcium targets and about one-half is due to events of a δ ray associated with an unscattered proton. The final value for the number of scattered particles in each bin was taken as the average of the results obtained by including and not including the first quadrant of the ΔX - ΔY plane, with an uncertainty estimated to be about $\pm 4\%$ in the absolute values of the total reaction cross sections. By a calculation following the expressions of Cverna,¹² we determined that the difference in number of δ rays produced in the three different calcium targets is only 3-4%. Since about 10% of the observed yield is estimated to be δ rays (when including the first quadrant), there is only a relative uncertainty of about $\pm 0.4\%$ due to δ rays for the three different total reaction cross-section measurements.

E. Extrapolation of integrated cross sections

The total reaction cross sections were obtained by integration over all angles of the inelastic differential cross section and by extrapolation of those cross sections to zero degrees as shown in Fig. 2. The integration was performed as a function of the scattering radius parameter IRAD by summing all observed scattered events for IRAD greater than or equal to each value. Only the cross section from IRAD = $5(\theta_{lab} = 10^\circ)$ and larger were used to determine the extrapolated values of the total reaction cross sections. The Coulomb plus nuclear elastic scattering cross

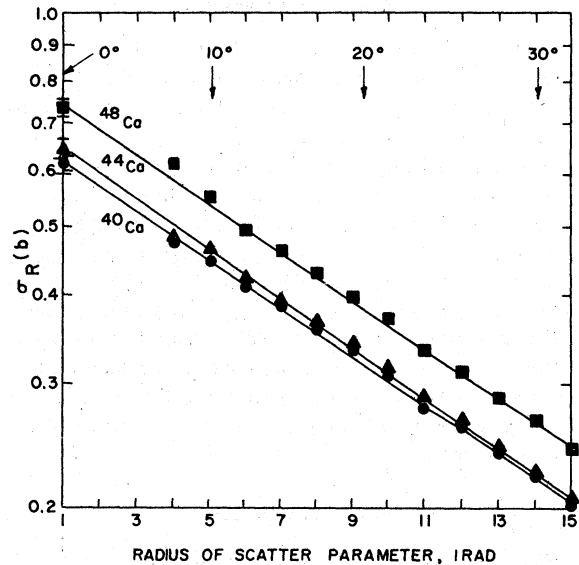


FIG. 2. Integrated reaction cross sections for the calcium isotopes versus the radius of scatter parameter IRAD (defined in the text). The total reaction cross sections determined by extrapolation to 0° (IRAD=1) are shown.

sections are very forward peaked at these energies and were negligible at angles greater than 10° as shown in Fig. 3. Because the solid angles subtended at the more forward angles are considerably smaller than those subtended at larger scattering angles, the yield from elastic scattering is found to contribute less than 0.1% to the total integrated observed yield for each of the three isotopes.

The angle-integrated cross sections presented

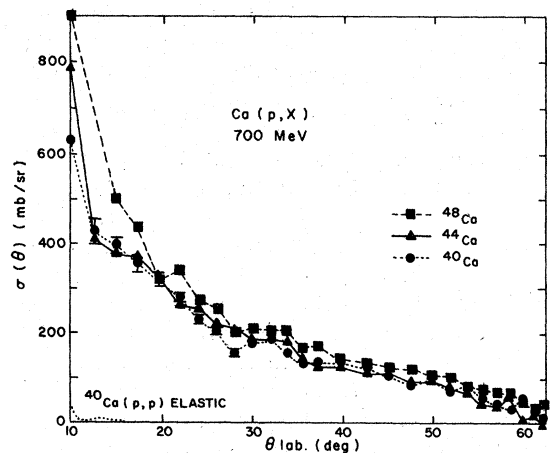


FIG. 3. Inelastic differential cross sections for the calcium isotopes from this experiment plus the elastic scattering cross section for ^{40}Ca at 1.04 GeV from Alkzov *et al.* (Ref. 13). Relative uncertainties are shown for the ^{40}Ca data points only, but are typical for all three isotopes.

in Fig. 2 are fit very well by straight lines on a semilog plot. Earlier workers^{4,5} who have measured total reaction cross sections on medium-weight nuclei have assumed that the angular distribution of inelastic products is approximately Gaussian, with a FWHM of about 25°–35° to extrapolate their data to zero scattering angle. Our differential cross sections (Fig. 3) appear more like two Gaussian peaks with FWHM values of about 20° and 40°, respectively, plus some definite forward-peaked yield. Because the solid angles at very forward angles become quite small, the total reaction cross section is dominated by the observed yield outside 10° (see Fig. 2). Rather than assume any specific shape for the angular distributions, we have chosen simply to fit the observed integrated cross sections with that function which goes through the experimental points most precisely. This is similar to the procedure adopted by Renberg *et al.*⁵ to extrapolate their integrated inelastic cross sections to obtain total reaction cross sections on other medium-weight nuclei at incident proton energies of 220–570 MeV. Our extrapolations to zero angle are estimated to be accurate to $\pm 4.0\%$ for the absolute values and to $\pm 2.0\%$ for the relative values of the total reaction cross sections. The yield outside the solid angle subtended by the large pair of multiwire chambers behind the target was estimated by extrapolation of the observed angular distributions to be less than 0.3% of the total yield for all three isotopes.

The various contributions to the relative and scale uncertainties are listed in Table I. The counting statistics are those of the total number of observed scattering events in the target-in and target-out runs after all of the various coincidence requirements and criteria had been satisfied. The total number of observed scattering events was about 9000 for each isotope, after subtracting target-out backgrounds of about 20–30%.

TABLE I. Uncertainties.

Scale	
1. Incident number of protons	$\pm (0.5)\%$
2. Target thickness	$\pm (0.5)\%$
3. δ -ray subtraction	$\pm (4.0)\%$
4. Extrapolation to zero	$\pm (4.0)\%$
	$\pm (5.7)\%$
Relative	
1. Counting statistics	$\pm (1.5)\%$
2. Extrapolation to zero	$\pm (2.0)\%$
3. δ -ray differences	$\pm (0.3)\%$
4. Dead-time losses	$\pm (0.0)\%$
	$\pm (2.5)\%$
Total: (rms)	$\pm (6.2)\%$

TABLE II. Results.

Isotope	Total reaction cross section
⁴⁰ Ca	614 mb
⁴⁴ Ca	643 mb
⁴⁸ Ca	736 mb

IV. RESULTS

The total reaction cross sections obtained from the extrapolations shown in Fig. 2 are listed in Table II. Although there are no other available measurements for the calcium isotopes at medium energies, we can compare our results with measurements for other medium-weight nuclei by using the simple $A^{2/3}$ dependence for the cross section which has been observed^{4,5} to be generally valid for measurements on targets over a wide range of the periodic table. Our result for ⁴⁰Ca agrees with the result of Chen *et al.*⁴ for Cu at 860 MeV to within 10% and with the more recent result of Renberg *et al.*⁵ for Fe at 570 MeV to within 5%. A simple energy dependence for the cross sections, based on a theoretical calculation discussed below, was assumed to make these comparisons.

In order to extract nuclear matter radii differences, we have performed theoretical calculations which take advantage of the geometrical nature of the cross section. These calculations were developed by one of us (D.J.E.) and are described in detail elsewhere.⁶ Basically, an eikonal propagator is used to solve the Lippman-Schwinger equation for scattering from an optical potential which is expressed to first order in the impulse approximation. Although the approximations of

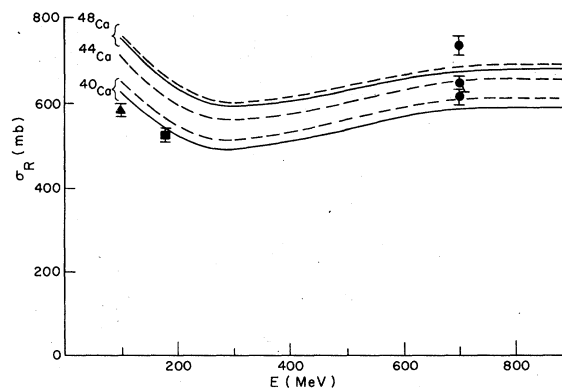


FIG. 4. Total reaction cross sections for the calcium isotopes. The solid lines represent calculations utilizing the Hartree-Fock densities from Negele (Ref. 14) and the dashed lines use densities from Varma and Zamick (Ref. 15).

the model rely on the short wavelength (0.7 fm) of the 700 MeV incident protons and the short mean-free-path of the protons in nuclear matter (about 1.3 fm), the model calculations have been found to be surprisingly accurate when compared with other available experimental measurements of total reaction cross sections for ^{12}C , ^{16}O , and ^{208}Pb targets at energies down to 100 MeV.⁶ The results of calculations with this model using nuclear matter density functions derived from a Hartree-Fock calculation¹⁴ and from analysis¹⁵ of 1 GeV proton elastic-scattering data are shown for ^{40}Ca , ^{44}Ca , and ^{48}Ca in Fig. 4 compared with the experimental results for ^{40}Ca of Kirby *et al.*¹⁶ at 90 MeV, Johansson *et al.*¹⁷ at 160 MeV, and our results at 700 MeV. It is seen that our results for ^{40}Ca and ^{44}Ca are reproduced accurately by the calculations based on the density function obtained for Varma and Zamick¹⁵ from their analysis of 1 GeV proton elastic scattering data for those two isotopes. However, the calculation underestimates our result for ^{48}Ca . The results for the nuclear matter rms radii differences obtained by adjusting the radius parameter in the theoretical calculations in order to reproduce our experimental results are presented in Table III.

The matter radii difference for ^{44}Ca - ^{40}Ca is consistent with the recent analysis performed by Varma and Zamick of the 1 GeV proton elastic-scattering data, the ^{48}Ca - ^{40}Ca matter radii difference is about twice as large as the 0.16 fm difference extracted by Varma and Zamick from the proton elastic scattering data. Although there have been earlier experimental measurements

TABLE III. Matter radii differences.

$\Delta R(44-40) = (0.05 \pm 0.09) \text{ fm}$
$\Delta R(48-40) = (0.36 \pm 0.09) \text{ fm}$

with 20–40-MeV ^{16}O ions¹⁸ and low-energy polarized protons¹⁹ which have implied even larger radii differences for ^{48}Ca - ^{40}Ca than do our measurements, this rather large result is somewhat puzzling. In Ref. 6 it is shown that reaction cross sections are determined by the density near a radius R_{eff} given by $\sigma_R = \pi R_{\text{eff}}^2$. (Our measured cross sections give $R_{\text{eff}} = 4.42 \text{ fm}$, 4.51 fm , and 4.84 fm for ^{40}Ca , ^{44}Ca , and ^{48}Ca , respectively.) In order to reproduce the measured cross sections, we find that the density at $R = R_{\text{eff}}$ must be approximately 15% of the central density. Therefore, more than anything else, our results imply a greater neutron density in ^{48}Ca near 4.84 fm than does the elastic scattering analysis. Because of the strong interest in knowing the nuclear sizes of the calcium isotopes, it would be worthwhile to see these measurements verified in another experiment.

Special thanks are due Dr. Alan Anderson for help in the preliminary stages of this experiment, to Bob Leskovec and Larry Hinkley, who provided technical support, and to members of the LAMPF staff who provided assistance and support during the running of the experiment. This work was supported by the U. S. Department of Energy.

*Present Address: Los Alamos Scientific Laboratory, Los Alamos, New Mexico 87545.

¹R. J. Glauber, in *High Energy Physics and Nuclear Structure*, edited by G. Alexander (North-Holland, Amsterdam, 1967), pp. 330–336.

²L. R. B. Elton, *Rev. Mod. Phys.* **30**, 557 (1958).

³R. W. Williams, *Phys. Rev.* **98**, 1387 (1955).

⁴F. F. Chen, C. P. Leavitt, and A. M. Shapiro, *Phys. Rev.* **99**, 857 (1955).

⁵P. V. Renberg, D. F. Measday, M. Pepin, P. Schwaller, B. Favier, and C. Richard-Serre, *Nucl. Phys.* **A183**, 81 (1972).

⁶D. J. Ernst, preceding paper, *Phys. Rev. C* **19**, 896 (1979).

⁷S. J. Wallace, *Ann. Phys. (N.Y.)* **78**, 190 (1973).

⁸H. B. Willard, B. D. Anderson, H. W. Baer, R. J. Barrett, P. R. Bevington, A. N. Anderson, H. Willmes, and Nelson Jarmie, *Phys. Rev. C* **14**, 1545 (1976).

⁹H. W. Bertini, M. P. Guthrie, and O. W. Hermann, Oak Ridge National Laboratory Report No. CCC-156, 1973

(unpublished).

¹⁰P. R. Bevington, B. D. Anderson, R. J. Barrett, F. H. Cverna, and A. N. Anderson, *Nucl. Instrum. Methods* **129**, 373 (1975).

¹¹P. R. Bevington and R. A. Leskovec, *Nucl. Instrum. Methods* **147**, 431 (1977).

¹²F. H. Cverna, Ph.D. dissertation, Case Western Reserve University, 1978 (unpublished).

¹³G. D. Alkhazov, S. L. Belostotsky, O. A. Domchenkov, Yu. V. Dotsenko, N. P. Kuropatkin, M. A. Schewaev, and A. A. Vorobyov, *Phys. Lett.* **57B**, 47 (1975); G. D. Alkhazov, T. Bauer, R. B. Beurtey, A. Boudard, G. Bruge, A. Chaumeun, P. Couvert, G. Cvizanovich, H. H. Duhm, J. M. Fontaine, D. Garetta, A. V. Kulikov, D. Legrand, J. C. Lugol, J. Saudinos, J. Thirion, and A. A. Vorobyov, *Nucl. Phys.* **A274**, 443 (1976).

¹⁴J. W. Negele, *Phys. Rev. C* **1**, 1260 (1970).

¹⁵G. K. Varma and L. Zamick, *Phys. Rev. C* **16**, 308 (1977).

¹⁶P. Kirby and W. T. Link, *Can. J. Phys.* **44**, 1847

- (1966).
- ¹⁷A. Johansson, V. Svanberg, and O. Sundberg, *Arkiv Phys.* 19, 527 (1961).
- ¹⁸M. C. Bertin, S. L. Tabor, B. A. Watson, Y. Eisen, and G. Goldring, *Nucl. Phys.* A167, 216 (1971).
- ¹⁹J. C. Lombardi, R. N. Boyd, R. Arking, and A. B. Robins, *Nucl. Phys.* A188, 103 (1972).